Non-hydrostatic modelling with AROME (and some properties of quasi-elastic systems)

Pierre Bénard

Centre National de Recherches Météorologiques
Toulouse, France
pierre.benard@meteo.fr

1 Introduction

The non-hydrostatic NWP model AROME is operational since December 2008. The dynamical kernel of AROME is part of a big NWP software library which also includes IFS, ARPEGE, ALADIN systems. After a short description of the AROME system, its behaviour and performances during these two years of routine operation will be reported in terms of practical output for forecasters. Besides, current works about quasi-elastic systems will be briefly presented, as a future possible option for the dynamical cores of the above-mentioned library.

2 Description of the AROME system

The AROME NWP system is a non-hydrostatic limited-area model with a 3D-var data-assimilation, used operationally at Météo-France for high-resolution forecasts since December 2008. The dynamical kernel and the data-assimilation packages are common with those of the limited-area ALADIN and the global ARPEGE models, used operationally at Météo-France at larger scales. The dynamical kernel is also common with the one of the global IFS model, used at ECMWF. However each particular application may use specific options (through logical switches) for its own purpose. For instance, ARPEGE and IFS have a 4D-var assimilation systems whereas ALADIN and AROME have a 3D-var system; similarly, from all these applications, AROME is the only one to use a non-hydrostatic dynamics operationally.

The dynamical kernel of AROME (Bénard *et al.*, 2010) is based on the fully compressible Euler Equations system cast in mass-based hybrid terrain-following coordinate (Laprise, 1992). The evolution is time-discretised with a semi-Lagrangian semi-implicit two-time levels scheme. The Helmholtz equation of the linear implicit problem is solved by a direct spectral solver based on a double Fourier transform in the horizontal. The Fourier transforms are used to compute horizontal derivatives, and vertical derivatives are computed with second-order finite-differences. A discretization with higher order finite-elements in the vertical is used in hydrostatic applications (ARPEGE, IFS) but is not available in the non-hydrostatic version.

The physical package of AROME is adapted from the Meso-NH meso-scale research model (Lafore *et al.*, 1998): The microphysics scheme is derived from the ICE3 scheme (Pinty and Jabouille, 1998), with five prognostic condensate species (liquid cloud, solid cloud, rain, graupel, snow). The turbulence parameterization scheme is a 1.5 order closure turbulence scheme with a prognostic TKE, adapted from Cuxart *et al.*, 2000. The surface scheme SURFEX is also derived from the Meso-NH environment. Since the AROME model is mostly designed for convection-permitting scales, no convection parameterization is used. The data-assimilation system is based on a 3D-var rapid-update cycle with a 3 hours

window. In comparison with ALADIN and ARPEGE, additional meso-scale observation data are assimilated in AROME (radar reflectivities and radial wind velocities, AMSU-A profiles, and higher density of AIREPS). More details on the physical and data-assimilation packages of AROME can be found in Seity *et al.*, 2011.

The operational suite of AROME consists in a continuous assimilation cycle from which a 30 h forecast is started every 6 hours. The horizontal grid increment is 2.5 km. A first version was implemented during the first 16 months of exploitation, until 6th April 2010. In this first version, the horizontal domain had 600×500 points along East and North directions respectively, as depicted in Fig. 1, and 41 irregularly spaced levels along the vertical. The time-step was set to 60 s. The AROME model was coupled to ALADIN (9 km grid-mesh) itself coupled to the operational stretched version of ARPEGE (15 km local grid-mesh). From 6th April 2010, with a new computer installed, the number of levels was set to 60, and AROME was directly coupled to ARPEGE, whose grid-spacing had been reduced to 10 km. A new version of AROME was implemented operationally on 24th November 2010 with a larger horizontal domain (750×720 points, still at 2.5 km grid-mesh), as depicted in Fig. 1. A new prognostic variable for hail was added with all relevant microphysics exchanges parameterized. More mesoscale observed data were finally used (seven additional Doppler radars, more AIREPS and IASI data assimilated). The coverage of assimilated radar data is shown in Fig. 2.

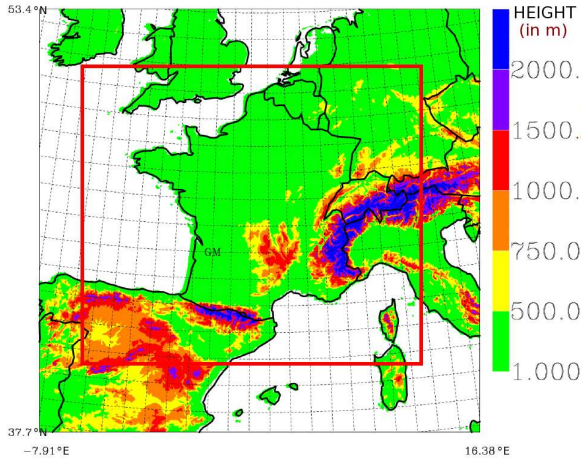

Figure 1: Domains of the first (inside red line) and second versions of AROME. Color shading : height of topography, in meters

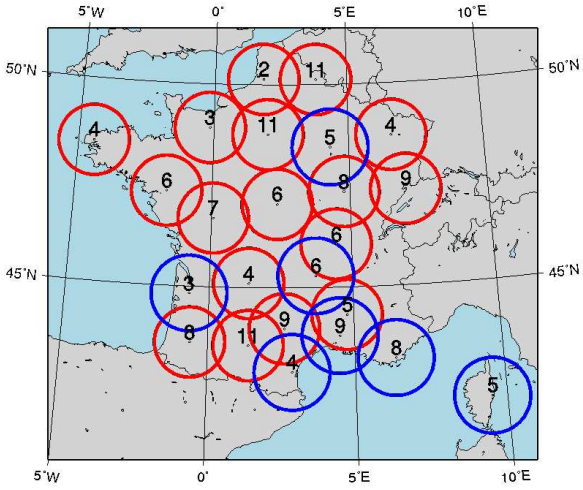

Figure 2: New assimilated radars (in blue). The numbers inside circles are the number of vertical sightings

3 Results and performances of the AROME system

As for all non-hydrostatic models, the changes and improvements against hydrostatic models outputs are limited to extreme events. In moderate conditions, the impact of non-hydrostatic processes and high-resolution remains weak, at least at kilometric scales. Therefore, although the routine objective scores indicate some added-value in the AROME forecasts (compared to its host models ALADIN or ARPEGE for instance), the signal is weak in average. Generally speaking, the improvement with AROME is more noticeable for temperature and humidity than for wind (not shown).

We choose to focus on two specific cases with severe weather. The first case is a recent Mediterranean heavy rain situation as those that commonly occur in the Languedoc region during Autumn (called

"cévenol" episode). The comparison of 1-hour accumulated precipitation forecast by AROME (left) and Radar reflectivities (right) is shown in Fig. 3. All AROME forecasts start at 00:00 UTC on the 30/10/2010, with forecast ranges of +6, +12, +18 and +24 hours. The structures and patterns of the precipitation field are quite well represented by the model (timing, bending of the bands, spreading of the large-scale structure). Smaller and weaker patterns occurring in other areas are also well captured. The correct location of precipitating areas from the beginning of the forecast may be attributed to the inclusion of related high-resolution data in the assimilation system and also to a smooth absorption of these relevant data through the rapid update cycle. However, even if the two fields shown in the panels are not directly comparable (instantaneous precipitations at varying heights and ground accumulated flux), this figure also illustrates a well identified under-estimation of weak precipitations rates in AROME forecasts.

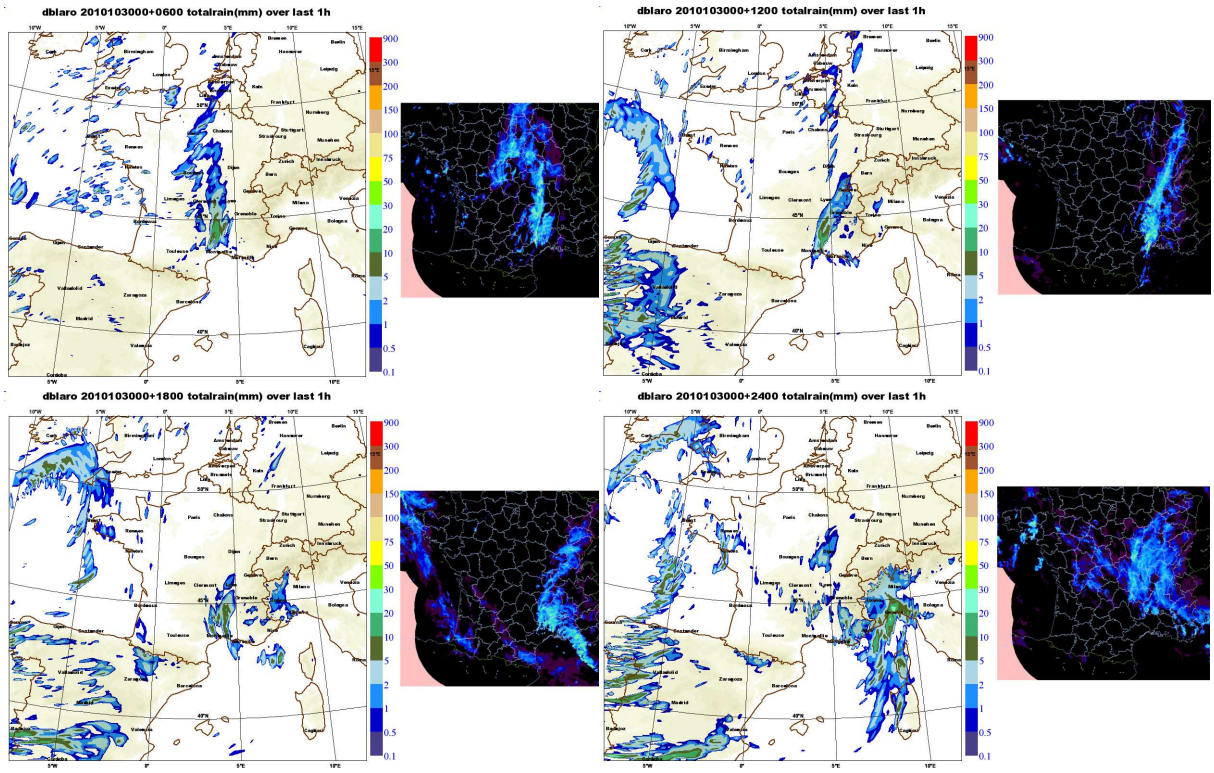

Figure 3: Maps of precipitations on 2010/10/30, at 0006, 1200, 1800 and 2400UTC. Left: AROME forecasts from 0000UTC for 1h accumulated precipitation at ground (in mm); right : instantaneous RADARS reflectivities

The Xynthia storm, that crossed the AROME domain on 2010/02/27 and 28, led to a severe sea flood on the Atlantic coast (30 deads) and strong winds over the Pyrénées mountains (1 dead) as can be seen from the map of the observed maximum gust for this event in Fig. 4.

The pattern of high values over the Pyrénées mountain is quite unusual (not to say very rare in such a context of Southerly flow) and the model predicted exceptional wind velocities. This was quite challenging for forecasters, who had to decide if they should trust the model or not. Other models confirmed the extreme character of the event, and the forecast was thus successful. The maximum gust was observed at the Pic du Midi observatory (209 km/h), and the event caused a lot of damages in the neighbourhood as well as in some valleys. In contrast, some areas located in the downwind flat region did experience relatively moderate winds during the whole event. A complex and transient evolution of the wind took place in the downwind side of the mountain range. Fig. 5 depicts the evolution of vertical velocity profiles observed above the Lannemezan VHF profiler. A wavy pattern with fast updrafts and downdrafts

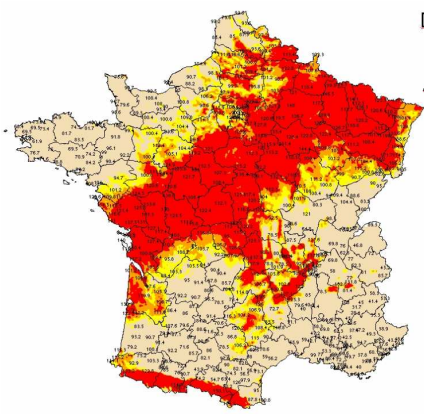

Figure 4: Map of maximum observed wind gust V for the Xynthia event 2010/02/27-28. Shadings : yellow : $V > 95$ km/h; orange : $V > 100$ km/h; red : $V > 105$ km/h

reflects the presence of waves (with associated divergence areas) quite far away (about 60 km) from the nountain ridge. AROME forecasts did capture these complex and mostly non-hydrostatic phenomena quite well, including the transient evolution of relatively windy and windless areas. The map of 10 m gust wind at 2100UTC on 2010/02/27 is displayed in Fig. 6 as forecast by AROME from 0000UTC illustrates the complex pattern field. The maximum gust predicted by AROME is 213 km/h, at the top of the ridge, while the maximum observed gust is 209 km/h at the Pic du Midi observatory, located at the very top of the mountain (there are no other verifying observation sites elsewhere on the top ridge of the mountain range). Areas of relative high and low values take place up to a hundred of km of the ridge in the downwind direction, and from this point of view, the AROME forecast was more accurate than the (hydrostatic) ALADIN forecast, bringing a significant added-value.

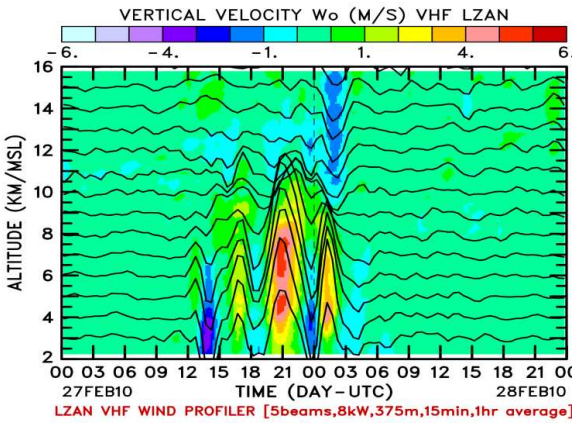

Figure 5: Evolution of observed vertical wind (in m/s) over Lannemezan (see red cross in Fig. 6).

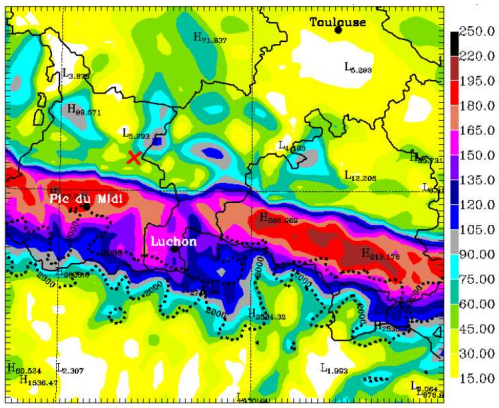

Figure 6: Map of the 10 m gust wind from AROME forecast starting at 2010/02/27 0000UTC for 21000UTC. Scaling in km/h. The red cross near the middle represents the location of Lannemezan.

Some results about the subjective evaluation of AROME by forecasters are presented now. The goals of this study is twofold: to evaluate AROME on specific real-case events, and to compare the merits of both AROME and ALADIN in operational use. The evaluation procedure is activated by forecasters

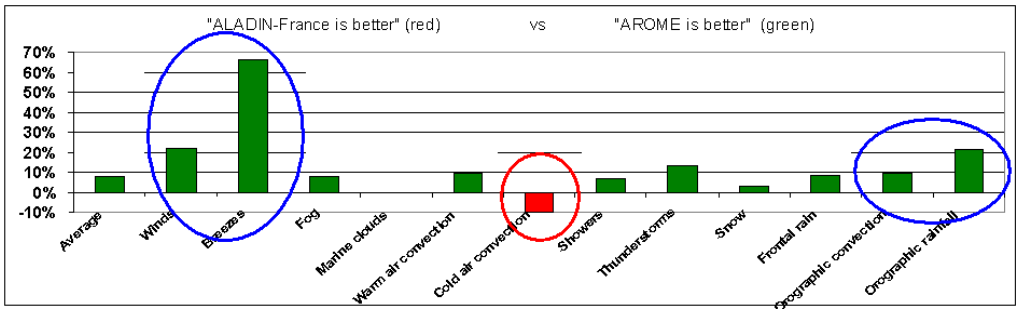

Figure 7: Synthesis of subjective comparison between AROME and ALADIN, by type of challenging event.

only on specific predicted events which appear as challenging for them and the models. Several types of challenges are defined (convective precipitations – orographically driven or not–, strong winds, snow, fog, ...). In order to make the subjective evaluation as fair and objective as possible, the indications given by the two models are logged before the event, then the verifying report and the performances are added after the event. Other questions about the a priori and a posteriori confidence to the model forecasts are also addressed. Concerning the performance itself, a synthesis of the comparison between AROME and ALDIN is shown in Fig. 7. A better behaviour is attributed to AROME in about 10% of the cases in average. There is a large variability of the relative performance as a function of the type of event. The best improvements brought by AROME are for wind-type and orographically driven events. Conversely, AROME behaves poorly with regards to cold-air convection, this is probably due to the well identified underestimate of predicted light precipitations.

Finally, a summary of the availability of the AROME forecasts is now given. Over some 700 days or so of operational use, 10 problems were reported, and among them, two led to an absence of forecast for one of the four daily runs. In one of these two cases the problem was not due to the model itself, but to the environment. The other one was linked to a too strong wind at the top of the domain. This was due to a drift in the data assimilation cycle, linked to the low density and high rejection of observed wind data in the stratosphere near the model top. The problem was rapidly solved by adding a slight restore-term toward the coupling model state in the very first uppermost levels of the model's domain top. The remaining problems mostly occured in the scheduler, because for peripheral reasons, files proved to be unavailable. Regarding these case, the forecast was most of the time made from an older analysis of the rapid-udpdate cycle, or by dynamical adaptation, with the up-to-date coupling data.

4 Some remarks about Quasi-Elastic systems

Although a fully-compressible dynamics using Euler Equations (EE) exists in the IFS/ARPEGE/ALADIN kernel, its formulation makes it difficult to implement high-order accurate finite-element discretizations in the vertical, and to modify the set of prognostic variables if desired. Among the possible avenues to circumvent these drawbacks, the use of a class of alternative equations systems is currently explored at ECMWF. This class of systems was recently proposed (Arakawa and Konor, 2009, AK09 hereafter) and may be viewed as the minimal modification to the EE system which allows a filtering of elastic waves. These systems have one less prognostic variable than the EE system, and therefore the pressure field is obtained through a diagnostic relationship. However, in opposition to anelastic systems, the approximation is not made around a stationary and horizontally homogeneous reference-state, but around a more general state close to the hydrostatic state.

In the EE system, the continuity equation writes:

$$\frac{\partial \rho}{\partial t} + \nabla(\rho \mathbf{V}) = 0, \tag{1}$$

where ρ the density and $\mathbf{V}$ the 3D wind vector. For the considered class of systems, the continuity equation is in written (i.e. approximated) as:

$$\frac{\partial \rho_h}{\partial t} + \nabla(\rho_h \mathbf{V}) = 0, \tag{2}$$

where ρ_h is an "hydrostatic density". Typically ρ_h will be defined by :

$$\frac{\partial p_h}{\partial z} = -\rho_h g \quad \text{and} \quad p_h = \rho_h RT; \tag{3}$$

here, p_h is therefore a modified hydrostatic pressure. Similar (but always close) variants are possible to define (ρ_h, p_h), thus leading to a class of systems. It is readily seen that in the limit of hydrostatic regimes, the continuity equation becomes exact, and the response of the system then approaches the response of the EE system. Moreover, in atmospheric flows at kilometric or hectometric scale, the relative deviation $(\rho - \rho_h)/\rho$ is very small and the approximation of the continuity equation is very good (in opposition to the approximation made in anelastic systems when the actual density significantly deviates from the specified basic-state density).

In the EE system, the continuous dispersion equation for linear eigenmodes around an isothermal resting state in Euclidian framework rotating f-plane is:

$$-(\nu^2 - f^2)(N^2 - \nu^2) - k^2c^2(\nu^2 - N^2) - c^2(m^2 + \mu^2)(\nu^2 - f^2) = 0, \tag{4}$$

where ν is the frequency, k (m) the horizontal (vertical) wavenumber, c the speed of sound, N the Brunt-Väïsälä frequency, and μ is a height-scale factor (see AK09). In the proposed system, the dispersion equation becomes

$$-(\nu^2 - f^2)N^2 - k^2c^2(\nu^2 - N^2) - c^2(m^2 + \mu^2)(\nu^2 - f^2) = 0. \tag{5}$$

The only modification with respect to the EE version is the absence of ν^2 in the second factor of the first term. However, this term which dispappears as a result of the approximation is not the leading term for the fast modes considered in this framework. Numerically, the frequency of a given mode (k, m) is therefore almost undistinguishable from its EE counterpart, and as a consequence, the structure and the frequency of eigenmodes are not distorted compared to EE ones. An argument developed at the end of Davies *et al.*, 2003 (D03 herefater) shows that this results holds for Rossby modes in the case of a rotating β-plane framework. Finally, the systems examined here are not subjected to the main theoretical objection against anelastic systems, also developed in D03, that is, the distorsion of Rossby waves propagation.

Since these systems are very close to the EE system, especially in the hydrostatic limit, and in the linear framework as far as elastic waves are not considered, they may be viewed as "quasi-elastic" systems (although they are termed "Quasi-Anelastic" in AK09).

We have shown that some of the variants of the proposed system lend themselves to a rather simple and direct formulation in mass-based vertical coordinates (very similar to Laprise, 1992), and that the

resulting equation system could be discretized in a very natural way in the framework of the IFS system (semi-Lagrangian, spectral...). Concerning the semi-implicit time-discretisation, here also, the system can be formulated in the same general framework as the very efficient one used in IFS (horizontally uniform and time-independent reference-state, separable problem, direct spectral solver, and precomputed vertical inverse operators).

Drawing from these inferences, the proposed system is promising. However, the main problem seems to be in the formulation and the solution of the diagnostic pressure equation. It appears to be much more cumbersome than in classical anelastic systems. The principle for deriving the pressure equation is similar to the anelastic case : the time derivative of the continuity equation must be combined with the divergence of the momentum equation. However, the presence of the time-derivative of ρ_h in (2) makes things much more complicated than in the anelastic case. To circumvent the problem, Arakawa and Konor, 2009, proposed as a practical trade-off, to keep this term formally as it is, and to compute it through a time-discrete estimate in the model. A full solution of the equation seems to be possible with an iterative 3D solver, but the efficiency of such a strategy remains open.

Besides, in order to establish if this system is sound and appropriate for IFS, it is necessary to determine the form of the energetic invariant, and the theoretical stability of the time-discrete system in presence of explicitly treated residuals (in the manner of Simmons *et al.* 1978). These points will be studied in the near future.

References

- Arakawa, A., and C. S. Konor, 2009: Unification of the anelastic and quasi-hydrostatic systems of equations. *Mon. Wea. Rev.*, **137**, 710-726.
- Bénard, P., 2010: Dynamical kernel of the Aladin-NH spectral limited-area model: Revised formulation and sensitivity experiments. *Mon. Wea. Rev.*, **136**, 155-169.
- Cuxart, J., P. Bougeault, and J.-L. Redelsperger, 2000, A turbulence scheme allowing for mesoscale and large-eddy simulations. *Q. J. R. Meteorol. Soc.*,**126**, 1-30.
- Davies, T., 2003: Validity of anelastic and other equation sets as inferred from normal-mode analysis. *Q. J. R. Meteorol. Soc.*,**129**, 2761-2775.
- Lafore,J. P., J. Stein, N. Asencio, P. Bougeault, V. Ducrocq, J. Duron, C. Fischer, P. Héreil, P. Mascart and V. Masson, et al., 2000 : The Meso-NH Atmospheric Simulation System. Part I: adiabatic formulation and control simulations. *Ann. Geophys.*, **16-1**, 90-109.
- Laprise, R., 1992: The Euler equations of motion with hydrostatic pressure as an independent variable. *Mon. Wea. Rev.*, **120**, 197-207.
- Pinty, J.-P. and P. Jabouille, 1998 : A mixed-phase cloud parameterization for use in a mesoscale non-hydrostatic model: simulations of a squall line and of orographic precipitations. *Conf. on Cloud Physics*, Everett, WA, Amer. Meteor. Soc., Preprints, 217-220.
- Seity, Y., P. Brousseau, S. Malardel, G. Hello, P. Bénard, F. Bouttier, C. Lac and V. Masson, 2011: The AROME-FRANCE convective scale operational model. *Mon. Wea. Rev.*, (in press).
- Simmons, A. J., B. Hoskins, and D. Burridge, 1978: Stability of the semi-implicit method of time integration. *Mon. Wea. Rev.*, **106**, 405-412.